### Multicriticality and quantum fluctuation in a generalized Dicke model

Youjiang Xu<sup>1</sup>, Diego Fallas Padilla<sup>1</sup>, and Han Pu<sup>1</sup>

Department of Physics and Astronomy and Rice Center for Quantum Materials, Rice University, Houston, Texas 77251-1892, USA



(Received 21 December 2020; accepted 6 October 2021; published 22 October 2021)

Quantum many-body systems that support high-order quantum phase transitions are quite rare. Here we consider an important generalization of the Dicke model in which an ensemble of multilevel atoms, instead of two-level atoms as in the conventional Dicke model, interact with a single photonic mode, and show that this generalized Dicke model can become multicritical. For a subclass of experimentally realizable schemes, multicritical conditions of arbitrary order can be expressed analytically in compact forms. As such, experiments can be readily designed to achieve quantum phase transition of desired order. We also calculate the atom-photon entanglement entropy for both critical and noncritical cases and find that the order of the criticality strongly affects the critical entanglement entropy: higher order yields stronger entanglement. Our work provides deep insight into quantum phase transitions and multicriticality.

#### DOI: 10.1103/PhysRevA.104.043708

#### I. INTRODUCTION

The Dicke model [1] is one of the most iconic models in quantum optics and quantum many-body physics. It describes an ensemble of two-level atoms interacting with a single photonic mode. When the atom-photon coupling strength exceeds a threshold, the system enters the superradiance phase via a second-order phase transition where the  $Z_2$  symmetry of the model is spontaneously broken, and the photonic mode is macroscopically populated. The Dicke model has been realized in various experimental settings, including quantum gases of neutral atoms [2–5], trapped ion systems [6], superconducting circuits [7–9], and solid-state systems [10]. Some of these experiments have probed the superradiant quantum phase transition (SQPT).

Real atoms, of course, possess complicated level structures. Even if we restrict ourselves to the ground-state manifold, a typical atom often features more than two levels. This motivates our current work to investigate an important generalization of the Dicke model where the two-level atoms are replaced by multilevel atoms. As we will show, the extra levels can be utilized to realize multicriticality in the SQPT. While multilevel generalizations of the Dicke model have been studied previously for various purposes [11-13], the possibility of multicriticality has not been investigated so far.

Theoretical studies [14–19] of multicriticality have been made after the first tricritical point, or third-order critical point, was discovered by Griffiths [20]. The results, to sum up, indicate that the phase diagram around the multicritical point possesses special geometry as several phase boundaries meet here, and more importantly, multicriticality modifies the scaling hypothesis and different order of criticality is associated with different universality class. However, despite the tricritical point being discovered in experiment from the very beginning, high-order criticality is rarely found in laboratories, making theoretical predictions difficult to verify.

It is therefore of crucial importance to provide a convenient experimental platform to achieve high-order criticality.

The difficulty in realizing high-order criticality lies in the fact that higher-order critical manifolds have lower dimension. According to the definition in Ref. [14], an nth-order critical manifold is the intersection of the (n-1)th-order critical manifolds, and the ordinary critical points are defined to be second order. Therefore the dimension of an nth-order critical manifold is (n-1) less than the dimension of the phase diagram. We will show that the generalized Dicke model we consider here exhibits remarkable features: (1) it provides plenty of experimentally tunable parameters to achieve high-order criticality and (2) the condition of the emergence of multicritical points of arbitrary order can be derived analytically. Quantum criticality features large quantum fluctuation which is usually characterized by a divergent correlation length. As our multicritical Dicke model describes a dimensionless system, we characterize the quantum fluctuation by the atom-photon entanglement entropy. We show that higher-order multicritical points are associated with a higher degree of entanglement, which provides insight into quantum phase transitions. Furthermore, the entanglement entropy can be extracted from the fluctuations of the photon quadrature operator.

#### II. MODEL

Our multicritical Dicke model describes N l-level atoms coupled with a single photonic mode of frequency  $\omega$ . The Hamiltonian can be written as  $(\hbar = 1)$ 

$$H = \omega a^{\dagger} a + \frac{g(a+a^{\dagger})}{2\sqrt{N}} \sum_{k=1}^{N} d^{(k)} + \epsilon \sum_{k=1}^{N} h^{(k)}, \qquad (1)$$

where a is the photon annihilation operator, dimensionless single-atom Hamiltonian h and dipole operator d act on the l inner states of the atoms, and g and  $\epsilon$  set the energy scales of the atom-photon interaction and the internal energy of the atoms, respectively. The conventional Dicke model is recovered if d and h are replaced by the two-level Pauli operators  $\sigma_x$  and  $\sigma_z$ , respectively. Note that we do not include the  $A^2$  term, which can lead to the no-go theorem for superradiance phase transition, in the Hamiltonian since we will consider Raman coupling between atomic levels, for which the  $A^2$  term is not relevant [21–24].

#### III. MEAN-FIELD PHASE DIAGRAM

We first discuss the multicritical Dicke model within the mean-field framework. The single-atom mean-field Hamiltonian  $H_{\rm MF}$  is obtained by replacing the bosonic operator a in H with a real number  $\epsilon \sqrt{N}\phi/g$ :

$$H_{\rm MF}/\epsilon = \kappa \phi^2 + \phi d + h,\tag{2}$$

where  $\kappa := \omega \epsilon/g^2$ . We denote the eigenstates of  $H_{\rm MF}$  as  $|k\rangle$ 's with eigenvalues  $\epsilon_k$  ( $k=1,2,\ldots,l$ ). We assume that  $|1\rangle$  is the nondegenerate ground state of  $H_{\rm MF}$ . In the Landau theory of phase transition, the  $\phi$  that minimizes  $\epsilon_1$ , denoted as  $\phi_{\rm min}$ , is defined to be the order parameter. For our system, if  $\phi_{\rm min}=0$ , the system is in the so-called normal phase; otherwise, it is in the superradiant phase.

The  $Z_2$  symmetry of Hamiltonian (1), which is spontaneously broken by the SQPT, manifests itself as H is invariant under the transformation  $a \to -a$ ,  $d \to -d$ ,  $h \to h$ . Given this symmetry, the mean-field ground-state energy can be written as a Taylor series in terms of  $\phi^2$ :  $\epsilon_1 = \sum_{k=0}^{\infty} c_k \phi^{2k}$ . An ordinary critical point is met when  $c_1 = 0$  and  $c_2 > 0$ . Generally, the nth-order critical manifold satisfies the condition  $c_1 = c_2 = \cdots = c_{n-1} = 0$  and  $c_n > 0$  (see Appendix A). These multicritical conditions can be expressed as equations in terms of pertinent parameters in d and d using perturbation theory. Treating d as the unperturbed Hamiltonian and d as the perturbation, we obtain d by carrying out the perturbation expansion to d the order. For example, the second-order perturbation expansion recasts d as

$$\sum_{k=2}^{l} \frac{|d_{1k}|^2}{h_{kk}} = \kappa,\tag{3}$$

and the fourth-order perturbation recasts  $c_2 = 0$  as

$$\sum_{k_1k_2k_3=2}^{l} \frac{d_{1k_1}d_{k_1k_2}d_{k_2k_3}d_{k_31}}{h_{k_1k_1}h_{k_2k_2}h_{k_3k_3}} = \sum_{k_1k_2=2}^{l} \frac{|d_{1k_1}|^2|d_{1k_2}|^2}{h_{k_1k_1}^2h_{k_2k_2}},$$
 (4)

and so on. Here the matrix elements are taken with respect to the eigenvectors of h. As we can arbitrarily pick an energy reference, we set  $h_{11} = 0$  and  $h_{kk} > 0$  for k = 2, 3, ..., l.

In general, the existence of the *n*th-order critical points requires at least n-1 tunable parameters spanning the phase diagram. For the multicritical Dicke model, the number of internal atomic levels l and the  $Z_2$  symmetry put constraints on the number of the tunable parameters. The  $Z_2$  symmetry requires the presence of a parity operator P which makes PdP = -d and PhP = h. Suppose the number of  $\pm 1$  in the eigenvalues of P is  $\frac{l \pm \delta}{2}$ . If we represent d and h as matrices using a set of common eigenvectors of h and P as the basis,

then h is diagonal and contains l tunable parameters, which are just the eigenvalues of h, whereas d must be in the form  $d = \begin{pmatrix} 0 & M \\ M^{\dagger} & 0 \end{pmatrix}$ , where M is a  $\frac{l-\delta}{2} \times \frac{l+\delta}{2}$  matrix. Now we have  $\frac{l^2-\delta^2}{2}+l$  parameters. Besides, we have to fix the l-1 relative phases between the common eigenvectors; also the physics would not change if we rescale  $\phi$  or H, or shift the zero-point energy. In the end, we have at most a  $(\mathcal{D} = (l^2 - \delta^2)/2 - 1)$ dimensional phase diagram. For example, for two-level atoms with l=2 as in the conventional Dicke model, we have  $\delta=0$ and  $\mathcal{D} = 1$ , which means only ordinary second-order critical points are allowed. In order to find multicriticality, we must have at least l=3. In the experimental work reported in Ref. [25], a tricritical point is identified in a spin-1 Bose gas subjected to spin-orbit coupling. This system can be recast into the form of the generalized Dicke model with l = 3 in the classical oscillator limit. In our previous work [26] (see also Ref. [27]), by introducing a staggered magnetic field to the two-level atoms, we show that this modified Dicke model exhibits tricriticality. This model can be regarded as a special case of the multicritical Dicke model under current consideration with l = 4.

Although the procedure of finding the multicritical condition of any order is straightforward under the perturbation approach outlined above, Eqs. (3) and (4) indicate that these equations quickly become very complicated as the order increases. Even numerical solutions to these equations may become impractical. However, we will show now that, for a subclass of the multicritical Dicke model, we can write down the multicritical conditions to arbitrary order in compact analytic forms. For this subclass, still under the representation where h is diagonal, only the super- and subdiagonal elements of the d matrix are nonvanishing, i.e.,  $d_{ij} = 0$  if  $|i - j| \neq 1$ . As a result,  $H_{\rm MF}$  takes a tridiagonal form, and hence we call this subclass the T class. For a T-class Hamiltonian, the nth-order critical condition is given by the simple form

$$|d_{k,k-1}|^2 = \kappa h_{kk} \quad \text{for } 2 \leqslant k \leqslant n. \tag{5}$$

To prove it, we denote, for a given l, the determinant of  $H_{\rm MF}$  as  $\zeta_l$ , which can be expressed as a Taylor series of  $\phi^2$ . If  $c_1 = c_2 = \cdots = c_{n-1} = 0$ , then  $\zeta_l \propto \phi^{2n}$ . We will now prove that  $\zeta_l \propto \phi^{2n}$  as long as Eq. (5) holds. To this end, we write down the recurrence relation for  $\zeta_k$  by exploiting the tridiagonal form of  $H_{\rm MF}$ :

$$\zeta_k = (h_{kk} + \kappa \phi^2) \zeta_{k-1} - \phi^2 |d_{k,k-1}|^2 \zeta_{k-2}.$$
 (6)

Under the condition of Eq. (5), we have  $\zeta_2 = \kappa^2 \phi^4$ ,  $\zeta_3 = \kappa^3 \phi^6$ . By induction, it is easy to prove  $\zeta_k = \kappa^k \phi^{2k}$  for k = 2, 3, ..., n. As a result,  $\zeta_l$  must be proportional to  $\phi^{2n}$  for  $n \leq l$ , which finishes the proof.

The experimental scheme for realizing a T-class Hamiltonian is illustrated in Fig. 1, using the F=2 hyperfine ground state of <sup>85</sup>Rb with cavity-assisted Raman transitions as an example. This scheme was proposed in Ref. [11] and realized in Ref. [12]. With one pair of Raman lasers as proposed in Ref. [11], the relative strength between  $d_{n,n-1} (\equiv d_{n-1,n})$ 's are fixed as  $(d_{12}, d_{23}, d_{34}, d_{45}) = (\sqrt{2}, \sqrt{3}, \sqrt{3}, \sqrt{2})$ , which will always be used in our numerical studies. With this d matrix, the multicritical conditions can be met by tuning  $h_{kk}$ 's, which represent the bare energies of the atomic internal states and

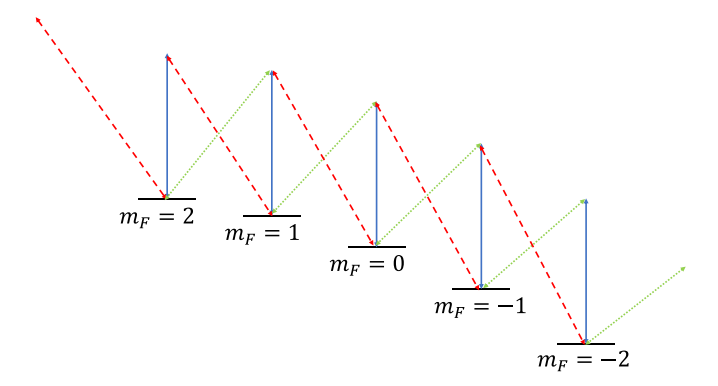


FIG. 1. The experimental scheme for realizing a T-class multicritical Dicke model. Using a pair of Raman beams with opposite circular polarization, as marked by the dashed and the dotted lines, respectively, and a linearly  $\pi$ -polarized cavity mode, as marked by the solid line, it is possible to couple adjacent hyperfine states of <sup>85</sup>Rb atoms through Raman coupling. By proper choice of the laser parameters, the coupling between "next-nearest" states (i.e., states with  $\Delta m_F = \pm 2$ ) through two Raman beams can be made to vanish because of the sum rule of the Clebsch-Gordan coefficients.

which can be tuned with external magnetic fields via the Zeeman shift or external microwave fields via the AC Stark shift [28–34]. In this scheme, up to fifth-order criticality can be realized. We set  $\kappa = 1$  in our numerical calculation; then the fifth-order critical point is located at  $(h_{22}, h_{33}, h_{44}, h_{55}) = (2, 3, 3, 2)$ .

In Fig. 2, we plot the phase diagrams of this T-class Hamiltonian. In Figs. 2(a) and 2(b), we show the change of the order parameter with respect to h, which is tuned around a tetracritical (i.e., fourth-order) point. This is done by setting  $h_{55}$  to be very large; hence we have effectively a

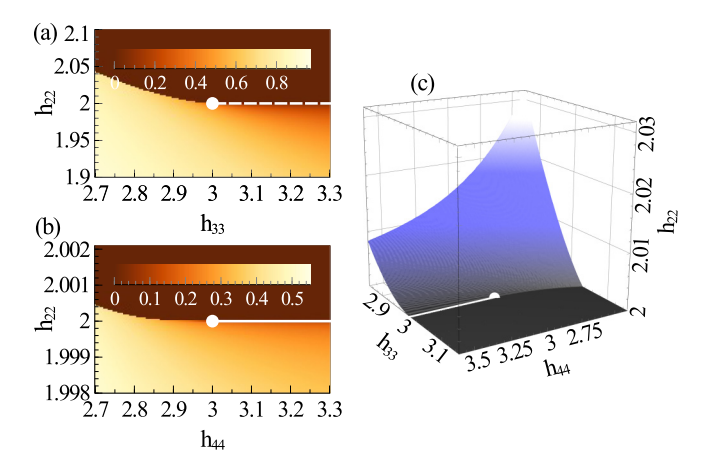


FIG. 2. (a, b) The mean-field phase diagram of a four-level T-class Hamiltonian around the fourth-order critical point. The color bar represents the order parameter  $\phi$ . The dashed line in (a) is an ordinary critical line while the solid line in (b) is a tricritical line. (c) The boundary that separates the normal phase (above) from the superradiant phase (below). The  $h_{22}=2$  plane is the critical manifold, with a tricritical line marked by a solid line. The curved surface is the first-order phase transition boundary. In all panels, we use a white dot to mark the fourth-order critical point.

four-level atomic system. The tetracritical point is located at  $(h_{22}, h_{33}, h_{44}) = (2, 3, 3)$  and is marked by the white dot in the graphs. In Fig. 2(a), we fix  $h_{44} = 3$  and vary  $h_{22}$  and  $h_{33}$ . The darker and lighter regions represent the normal and the superradiant phases, respectively. The ordinary second-order critical line is marked by the white dashed line which is a straight line with  $h_{22} = 2$  and  $h_{33} > 3$ . The phase boundary to the left of the tetracritical point is of first order. In Fig. 2(b), we fix  $h_{33} = 3$  and vary  $h_{22}$  and  $h_{44}$ . Here the straight solid line with  $h_{22} = 2$  and  $h_{44} > 3$  is a tricritical line, which joins the first-order boundary at the tetracritical point. In Fig. 2(c), we show the boundary surface between the normal (above the surface) and the superradiant phase (below the surface) in the full three-dimensional parameter space. This boundary surface contains two parts: a flat part at plane representing the second-order critical manifold and a curved part representing the first-order surface. The tricritical line and the tetracritical point are marked by the white solid line and the white dot, respectively.

#### IV. QUANTUM FLUCTUATION AND ENTANGLEMENT

Having discussed the mean-field phase diagram, we now turn our attention to the quantum fluctuation and the entanglement properties of the model. By shifting the bosonic operator by the mean-field order parameter,  $b := a - \epsilon \sqrt{N}\phi_{\min}/g$ , Eq. (1) is rewritten as

$$H = \omega b^{\dagger} b + \frac{g(b^{\dagger} + b)}{2\sqrt{N}} \sum_{k=1}^{N} D^{(k)} + \sum_{k=1}^{N} H_{\text{MF}}^{(k)}, \tag{7}$$

where the shifted dipole operator is  $D:=d+2\kappa\phi_{\min}$ . Without loss of generality, the atomic states can be expressed in terms of an orthonormal basis consisting of completely symmetrized Fock states  $|\chi\rangle$ , where  $\chi$  is a vector whose components  $\chi_i$  denote the number of atoms occupying  $|i\rangle$ , the ith eigenstate of  $H_{\mathrm{MF}}$ . Consequently, the last term in Eq. (7) is diagonal in this basis,  $\langle \chi | \sum_{k=1}^N H_{\mathrm{MF}}^{(k)} | \chi \rangle = \sum_{i=1}^l \epsilon_i \chi_i$ . The nonzero matrix elements of  $\sum_{k=1}^N D^{(k)}$  under the basis  $|\chi\rangle$ 's are

$$\langle \chi | \sum_{k=1}^{N} D^{(k)} | \chi \rangle = \sum_{k=1}^{N} \chi_k D_{k,k},$$
 (8)

$$\langle \chi^{i,j} | \sum_{k=1}^{N} D^{(k)} | \chi \rangle = \sqrt{\chi_j(\chi_i + 1)} D_{i,j}, \tag{9}$$

where  $|\chi^{i,j}\rangle$  is the very state containing one more atom in  $|i\rangle$  and one less atom in  $|j\rangle$  than  $|\chi\rangle$ . As long as we are interested in the low-energy states, we can assume that most atoms occupy the mean-field ground state  $|1\rangle$ , i.e.,  $\chi_1 \sim N$  and  $\chi_k = o(N)$  for k = 2, 3, ..., l. In the limit  $N \to \infty$ , we can then express  $H = H_{\text{eff}} + N\epsilon_1 + o(1)$ , and the low-energy effective Hamiltonian  $H_{\text{eff}}$  is quadratic in b and new bosonic operators  $b_2, b_3, ..., b_l$ :

$$H_{\text{eff}} = \omega b^{\dagger} b + \sum_{i=2}^{l} \left[ \omega_{i} b_{i}^{\dagger} b_{i} + \frac{g|D_{1,i}|}{2} (b + b^{\dagger})(b_{i} + b_{i}^{\dagger}) \right], \tag{10}$$

where  $b_i$  is defined by  $b_i|\chi^{1,i}\rangle = \sqrt{\chi_i}|\chi\rangle$ , and  $\omega_i = \epsilon_i - \epsilon_1$ . In deriving Eq. (10), we have used  $D_{1,1} = 0$ , which results from the stationarity of the mean-field energy  $\partial_\phi \epsilon_1 = 0$ . Because the leading term in the asymptotic series of H is the mean-field energy  $N\epsilon_1$ , it confirms that the mean-field theory determines the exact phase diagram in the thermodynamic limit as long as the asymptotic expansion is valid. The validity of the expansion can be verified self-consistently; i.e., it is valid as long as  $\sum_{i=2}^{l} \langle b_i^\dagger b_i \rangle \ll N$ , where the expectation value is taken with respect to the low-energy states.

To find the ground state of  $H_{\rm eff}$ , which describes the lowenergy quantum fluctuations above the mean field, we can transform  $H_{\rm eff}$  into a Hamiltonian describing an l-dimensional harmonic oscillator,

$$H_{\text{eff}} = \frac{1}{2} \sum_{j,k=1}^{l} \left( P_j \delta_{jk} P_k + X_j \Omega_{jk}^2 X_k \right) - \frac{1}{2} \sum_{k=1}^{l} \omega_k, \tag{11}$$

where  $P_k = \sqrt{\frac{\omega_k}{2}}(b_k - b_k^{\dagger})$  and  $X_k = \frac{1}{\sqrt{2\omega_k}}(b_k + b_k^{\dagger})$  are canonical momentum and position operators as linear combinations of  $b_k$  and  $b_k^{\dagger}$ . Here we have denoted  $b_1 \equiv b$  and  $\omega_1 \equiv \omega$ . The squared eigenfrequencies  $\lambda^2$  of the harmonic oscillator are given by the eigenvalues of the matrix  $\Omega^2$ , whose nonzero matrix elements are given by

$$\Omega_{kk}^2 = \omega_k^2 \quad \text{for } k = 1, 2, \dots, l,$$
 (12)

$$\Omega_{1k}^2 = |D_{1,k}| \sqrt{\omega \omega_k} \quad \text{for } k > 1.$$
 (13)

We calculate the spectrum of  $H_{\rm eff}$  (for details, see Appendix B). We note that only the lowest eigenvalue of  $\Omega^2$ , denoted as  $\lambda_1^2$ , can be zero. The asymptotic expansion is valid when  $\lambda_1^2 > 0$ ; otherwise, the fluctuation blows up. So the equation  $\lambda_1^2 = 0$  indicates the quantum criticality, which coincides with the mean-field critical condition Eq. (3) as required by self-consistency. The ground-state wave function of  $H_{\rm eff}$  is an l-dimensional Gaussian, from which the atom-photon entanglement entropy can be calculated straightforwardly:

$$S = \frac{\gamma}{e^{\gamma} - 1} - \ln(1 - e^{-\gamma}), \tag{14}$$

$$\gamma \equiv \cosh^{-1}\left(\frac{\Omega_{11}M_{11}/\det\Omega + 1}{\Omega_{11}M_{11}/\det\Omega - 1}\right),\tag{15}$$

where  $M_{11}$  is the (1, 1)-minor of the matrix  $\Omega$ . Here S is the von Neumann entropy of the reduced density matrix for either the atomic or the photonic modes. At the critical points, the gap closes  $(\lambda_1 = 0)$ , so det  $\Omega = 0$ ,  $\gamma = 0$ , and S diverges. Near the critical points,  $\gamma$  is small, so approximately we have  $S = 1 - \ln \gamma$ , which indicates a logarithmic divergence approaching the critical point. Furthermore, one can readily show (see Appendix A) that

$$\Omega_{11}M_{11}/\det\Omega = -\langle (b+b^{\dagger})^2 \rangle \langle (b-b^{\dagger})^2 \rangle, \tag{16}$$

where  $(b \pm b^{\dagger})$  are cavity photon quadrature operators. As a result, we draw a remarkable conclusion that the atomphoton von Neumann entanglement entropy of this system can be extracted from the measurement of photon quadrature fluctuations. This conclusion extends the previous results on quantifying the entanglement between two-mode systems [35,36] as multiple modes are involved in the current model.

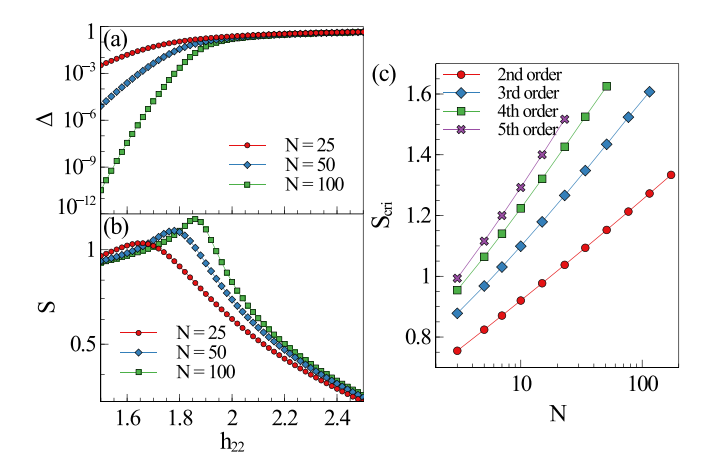


FIG. 3. (a) The gap  $\Delta$  between the ground state and the first excited state, and (b) the ground-state entropy S, of the two-level Dicke model with  $d_{12} = \sqrt{2}$  for different atom number N.  $\Delta$  exponentially decreases when  $h_{22}$  moves deep into the superradiant phase. (c) Critical atom-photon entanglement entropy  $S_{\rm cri}$  plotted against the atom number N for T-class Hamiltonians with different orders of criticality. Different orders of criticality are achieved by first setting  $(h_{33}, h_{44}, h_{55}) = (3, 3, 2)$ , and then tuning some  $h_{kk}$  to very large values. For example, to achieve the tricriticality, we set  $h_{44}$  and  $h_{55}$  to be large.

Finally, we examine the entanglement entropy at the critical points away from the thermodynamic limit with finite N. A similar calculation for the conventional Dicke model and more general two-mode Hamiltonian is carried out by Vidal et al. [37,38]. We numerically calculate the finite-N critical entropy for the T-class Hamiltonians. In the thermodynamic limit, the ground state is nondegenerate in the normal phase while it is doubly degenerate in the superradiant phase, and the excitation gap closes at the phase boundary and remains closed in the superradiance region. For finite N, however, the gap  $\Delta$  does not close, but rather decreases exponentially when we move deeper into the superradiant region [see Fig. 3(a)]. Therefore, the phase boundaries and the critical manifolds in a finite system cannot be determined unambiguously by the gap. Instead, we define the critical point for finite N as the point at which the atom-photon entanglement entropy S reaches a local maximum [see Fig. 3(b)], and the corresponding entropy is identified as the critical entropy  $S_{cri}$ . In Fig. 3(c), we plot  $S_{cri}$ against N at critical points with different order of criticality for the T-class Hamiltonians. Asymptotically, we have  $S_{\rm cri} \sim$  $s_0 + s_1 \ln N$ . Figure 3(c) shows that higher-order criticality is associated with greater critical entanglement entropy.

#### V. CONCLUSION

We replace the two-level atoms in the conventional Dicke model with l-level atoms and study the superradiance phase transition in the modified model. The increased number of tuning parameters for l>2 leads to the emergence of multicriticality whose order can be controlled. The phase diagram and the multicritical conditions can be obtained from the mean-field theory. For a subclass of this multicritical Dicke model, which can be readily realized experimentally, we show that the multicritical conditions of arbitrary order can be ex-

pressed analytically in compact forms, which facilitates the realization of phase transition of desired orders. The noncritical atom-photon entanglement entropy of the multicritical Dicke models in the thermodynamic limit can be calculated analytically through an asymptotic expansion of the Hamiltonian, and can be measured in experiments from cavity field quadrature fluctuations. The entropy diverges logarithmically when approaching the critical point. The entropy at the critical points for finite number of atoms is calculated numerically and is found to have a  $\ln N$  scaling. We found that the critical entropy increases when the order of criticality increases. Our work provides deep insights into the physics of quantum phase transition and multicritical points, whose realization is typically very challenging in other contexts. In this work, we have neglected dissipation, which in practice is inevitable and can play important roles in determining the critical and multicritical behaviors of the system. The study of the effects of dissipation is currently under way.

#### **ACKNOWLEDGMENTS**

We acknowledge support from the NSF and the Welch Foundation (Grant No. C-1669).

# APPENDIX A: MULTICRITICAL CONDITIONS IN SINGLE-PARAMETER LANDAU THEORY OF PHASE TRANSITIONS

Landau theory of phase transitions is the basic theoretical framework to describe phase transitions involving spontaneous symmetry breaking. For phase transitions breaking a  $Z_2$  symmetry with a single order parameter  $\phi$ , the free energy F is an even function of the order parameter, analytic at  $\phi = 0$ , expressed by a Taylor series containing only the even power terms:

$$F(\phi) = \sum_{n=0}^{\infty} c_n \phi^{2n}.$$
 (A1)

The phase is determined by the global minimums  $F(\phi_{\min})$  of  $F(\phi)$ . When  $\phi_{\min} \neq 0$ , the system is in the phase where the  $Z_2$  symmetry is spontaneously broken, because at least there are two  $\phi_{\min}$ 's with opposite signs. When  $\phi_{\min} = 0$ , the system is in the phase where the symmetry is preserved. There is a phase boundary between the two phases. In particular, the part of phase boundary crossing which  $\phi_{\min}$  changes continuously is the critical manifolds. At least two global minimums merge into one at a critical point. The intersection between several critical manifolds is defined to be the multicritical manifold. In general, An nth-order critical manifold is the intersection of (n-1)th critical manifolds, and the ordinary critical manifolds are defined to have order 2. We are going to analyze the multicritical manifolds induced by  $F(\phi)$ .

First, let us discuss the simplest case frequently met in textbooks where all  $c_n$ 's are zero except  $c_1$  and  $c_2$ . In order that F has a global minimum and the system is stable, we must have  $c_2 > 0$ . Now, F can be written as

$$F = c_2 \left(\phi^2 + \frac{c_1}{2c_2}\right)^2 - \frac{c_1^2}{4c_2},\tag{A2}$$

which has two global minimums at  $\phi = \pm \sqrt{-\frac{c_1}{2c_2}}$  if  $c_1 < 0$ , and has one global minimum at  $\phi = 0$  if  $c_1 > 0$ . Therefore, the equation for the critical manifold, where two global minimums merge into one, is given by  $c_1 = 0$ .

In the case that F is quadratic in  $\phi^2$ , there are at most two global minimums. There is no more critical manifold that can intersect with the one specified by  $c_1 = 0$ , so there is no critical manifold whose order is greater than 2. To have two or more critical manifolds that intersect, we must have at least three minimums. The simplest F that supports three local minimums is a cubic function in  $\phi^2$ . To guarantee the stability, the coefficient  $c_3$  must be positive. F may have a local minimum at  $\phi = 0$  due to the symmetry. When  $\frac{dF}{d\phi^2}|_{\phi=0} > 0$ ,  $\phi = 0$  must be a local minimum. We know

$$\frac{dF}{d\phi^2} = c_1 + 2c_2\phi^2 + 3c_3\phi^4,\tag{A3}$$

so when  $c_1 > 0$ ,  $\phi = 0$  is a local minimum. F may also have two local minimums at  $\phi = \pm \phi_0$ , where  $\phi_0^2 > 0$  is the larger solution of the equation  $\frac{dF}{d\phi^2}|_{\phi^2=\phi_0^2}=0$ . Thus,

$$\phi_0^2 = \frac{\sqrt{c_2^2 - 3c_1c_3} - c_2}{3c_3},\tag{A4}$$

with the condition  $c_3>0$ . To make  $\phi_0^2>0$ , it is required that either  $c_1<0$ , or  $c_2<0$  and  $c_2^2\geqslant 3c_1c_3$ . In addition, when  $c_1=0$  and  $c_2\geqslant 0$ ,  $\phi=0$  is a minimum. In conclusion, the free energy F has (1) a single local minimum at  $\phi=0$ , which is also the global minimum, if  $c_1>0$  and  $c_2^2<3c_1c_3$ , or  $c_1\geqslant 0$  and  $c_2\geqslant 0$ ; (2) double local minimums at  $\phi=\pm\phi_0$ , which are also the global minimums, if  $c_1<0$ , or  $c_1=0$  and  $c_2<0$ ; and (3) three local minimums at  $\phi=\pm\phi_0$ , if  $c_1>0$  and  $c_2<0$  and  $c_2^2\geqslant 3c_1c_3$ .

In the third case above, to determine where the global minimum is, we need to evaluate F at  $\phi=0$  and  $\phi^2=\phi_0^2$ , respectively. The calculation can be simplified by noticing that when F gets three global minimums, it must take the form

$$F = c_0 + c_3 \phi^2 (\phi^2 - \phi_0^2)^2.$$
 (A5)

By identifying this formula with the Taylor expansion of F, we get

$$-2\phi_0^2 c_3 = c_2, (A6)$$

$$0 = c_2^2 - 4c_1c_3$$

0

$$c_2 + 2\sqrt{c_1 c_3} = 0. (A7)$$

In the phase diagram, this equation specifies the triple line, where three phases coexist. When  $c_2 + 2\sqrt{c_1c_3} > 0$ , the single global minimum locates at  $\phi = 0$ , and when  $c_2 + 2\sqrt{c_1c_3} < 0$ , the double global minimums locate at  $\phi = \pm \phi_0$ .

With all of the discussion above, we can establish the phase diagram (Fig. 4) for the free energy as a cubic polynomial. First of all, it is a two-dimensional phase diagram with parameters  $c_1$  and  $c_2$ . There is a continuous phase transition boundary, which is also the critical line, whose shape is determined by the equation  $c_1 = 0$  and  $c_2 \ge 0$ , and there is a

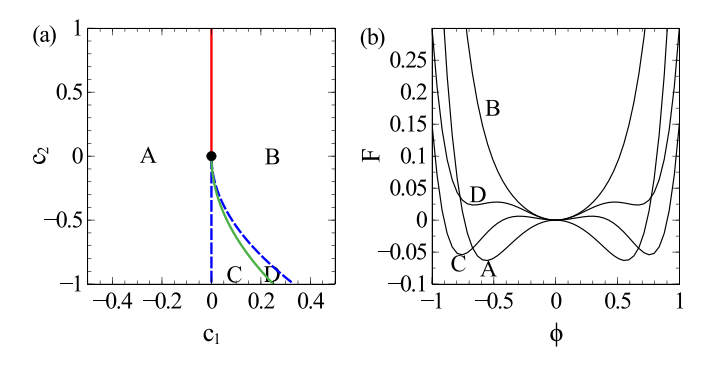


FIG. 4. (a) The phase diagram associated with a free energy F that is a cubic polynomial in  $\phi^2$ . The solid lines are the phase boundaries. The region to the left of the boundary marked by A and C is the symmetry-breaking phase and the right marked by B and D is the symmetry-preserving phase. The red solid line in the region  $c_2 > 0$  is the critical line. The green solid line in the region  $c_2 < 0$  is the triple line where three phases coexist. Regions C and D within the blue dashed line have three local minimums in the free energy. The black dot in the center is the tricritical point. (b) Typical plots of F against  $\phi$  for different regions shown in (a).

discontinuous phase transition boundary, which is also the triple line, whose equation is  $c_2 + 2\sqrt{c_1c_3} = 0$  and  $c_2 < 0$ . The two boundaries smoothly join together at the point  $c_1 = c_2 = 0$ , in the sense that the derivative  $\frac{dc_1}{dc_2}$  approaches zero when we approach the point  $c_1 = c_2 = 0$  along either line. The boundary divides the phase diagram into two half planes. The half plane contains the region  $c_1 < 0$  and represents the symmetry-breaking phase and the other half plane represents the symmetry-preserving phase.

The intersection of the continuous and discontinuous phase boundaries, located at  $c_1 = c_2 = 0$ , is the tricritical point. It can be understood by modifying the free energy with an additional term  $c_{1/2}\phi$  which breaks the  $Z_2$  symmetry. With such a linear term in the free energy, it becomes difficult to write down the analytical expressions for the minimums of F, but we can still analyze the geometry of the phase diagram. First, the maximum number of the local minimums of F is still three, because a linear term would only shift the function  $\frac{dF}{d\phi}$  by a constant. Then, let us mark the locations of the three local minimums by  $\alpha$ ,  $\beta$ , and  $\gamma$ , if they exist, with the condition  $\alpha < \beta < \gamma$ . Now, without the  $Z_2$  symmetry,  $\beta$  is not necessarily zero, and  $\alpha$  may be different from  $-\gamma$ . By properly adjusting  $c_{1/2}$ , it is possible to make  $\alpha$  and  $\beta$  the global minimums that merge into one minimum at a critical line, or to make  $\beta$  and  $\gamma$  the global minimums that merge at another. These two new critical lines will join the critical line on the  $Z_2$ -symmetric surface at the point  $c_1 = c_2 = 0$ , where the three global minimums merge simultaneously. Thus, in the extended phase diagram including the additional variable  $c_{1/2}$ , it is manifested that the point  $c_1 = c_2 = 0$  is indeed the tricritical point.

Next, we consider the case where F is a polynomial of  $\phi^2$  whose degree is  $\xi$ . Again, to ensure the stability, the coefficient  $c_{\xi} > 0$ . In general, it is impossible to write down the analytical expressions for the minimums of F; however, it is possible to gain insight into the topology of the minimums, that is, how the minimums merge and split, which

remarks the criticality and multicriticality. In the cubic case, the third-order critical point is the point where three global minimums merge, then in general, the nth-order critical point should be the point where n global minimums merge, if we allow the broken  $Z_2$  symmetry. This definition is consistent with the previous one, because when we have n global minimums, we can select n groups of n-1 minimums to merge into (n-1)th-order critical manifolds, and the intersection of these n lower-order critical manifolds is the point where all of the n minimums merge, and thus is the nth-order critical point. n has at most n global minimums, so it can support at most a n theorem critical point. When a general polynomial n (where the prime is for the broken n symmetry) of n with degree n with degree n has n n n n global minimums, it can always take the form

$$F' = \prod_{k=1}^{n} (\phi - a_k)^2 \prod_{l=1}^{\xi - n} (\phi - b_l)(\phi - b_l^*) + F_0', \quad (A8)$$

where  $a_k$ 's are the locations of the n minimums, n + n' is the degree of F' in terms of  $\phi$ ,  $b_l$ 's are some complex numbers with nonvanishing imaginary part, and  $F'_0$  is the value F' takes at the minimums. When the n minimums in Eq. (A8) merge, the  $a_k$ 's approach the same value A simultaneously, and now F' takes the form

$$F' = (\phi - A)^{2n} \prod_{l=1}^{\xi - n} (\phi - b_l)(\phi - b_l^*) + F_0'.$$
 (A9)

Therefore, we derive another criterion for the multicriticality, that is, around an *n*th-order critical point  $\phi = A$ , the free energy should be a power function of  $\phi - A$  to the (2n)th, or  $F' - F'_0 \propto (\phi - A)^{2n}$ . In the case A = 0, we have

$$F = \phi^{2n} \prod_{l=1}^{\xi-n} \left( \phi^2 + \left| b_l^2 \right| \right) + F_0'. \tag{A10}$$

Accordingly, the equation to determine the *n*th-order critical manifold in the phase diagram is

$$c_1 = c_2 = \dots = c_{n-1} = 0,$$
 (A11)

with

$$c_n, c_{n+1}, \dots, c_{\xi} > 0.$$
 (A12)

In this case, the *n*th-order critical manifold is the boundary of the (n-1)th-order critical manifold.

In general, F is not a polynomial but contains arbitrarily high-order terms. The previous argument which leads to Eq. (A11) still holds, however, because now we have infinite parameters  $c_n$ ,  $c_{n+1}$ , ... that need to satisfy inequality (A12), which seems impractical. The problem can be circumvented by considering only very small values of  $\phi$ . Now, as long as  $c_n > 0$ , the higher-order terms can be neglected without changing the behavior of F in a sufficiently small neighborhood of  $\phi = 0$ , which is implied by a continuous phase transition. Therefore, we can say the nth-order critical condition for a free energy F taking the form of Eq. (A1) is given by Eq. (A11) together with

$$c_n > 0. (A13)$$

Equation (A11) indicates that an *n*th-order critical manifold has the dimension  $\mathcal{D} - n + 1$  where  $\mathcal{D}$  is the dimension of the phase diagram.

## APPENDIX B: SOLVING THE LOW-ENERGY EFFECTIVE HAMILTONIAN OF THE GENERALIZED DICKE MODEL

We start from Eq. (10):

$$H_{\text{eff}} = \frac{1}{2} \left( \sum_{j,k=1}^{l} P_j \delta_{jk} P_k + X_j \Omega_{jk}^2 X_k \right) - \frac{1}{2} \sum_{k=1}^{l} \omega_k, \quad (B1)$$

where  $\Omega^2$  is an  $l \times l$  matrix whose diagonal elements are given by

$$\Omega_{kk}^2 = \omega_k^2, \quad k = 1, 2, \dots, l,$$
 (B2)

and the nonzero off-diagonal elements are

$$\Omega_{1k}^2 = g|D_{1,k}|\sqrt{\omega\omega_k},\tag{B3}$$

$$\Omega_{k1}^2 = \Omega_{1k}^2, \tag{B4}$$

where k = 2, 3, ..., l. The spectrum of  $H_{\text{eff}}$  is solely determined by  $\Omega^2$ . By diagonalizing  $\Omega^2$ ,  $H_{\text{eff}}$  can be represented as a sum of l independent one-dimensional harmonic oscillators, whose eigenfrequencies are equal to the eigenvalues  $\lambda_i$  of  $\Omega$ ,

i = 1, 2, ..., l. So the eigenvalues  $E_{\text{eff}}$  of  $H_{\text{eff}}$  are given by

$$E_{\text{eff}}(n_1, n_2, \dots, n_l) = \sum_{i=1}^{l} n_i \lambda_i + \frac{1}{2} (\lambda_i - \omega_i),$$
 (B5)

where the non-negative integers  $n_i$  are the excitation number for each of the l independent one-dimensional harmonic oscillators. And the ground-state wave function of  $H_{\rm eff}$  is given by

$$\Phi(\mathbf{X}) = \left(\frac{\det \Omega}{\pi^l}\right)^{1/4} \exp\left(-\frac{\sum_{j,k=1}^l \Omega_{jk} X_j X_k}{2}\right), \quad (B6)$$

which is the product of the ground-state wave function of the *l* independent one-dimensional harmonic oscillators.

Information on the eigenvalues  $\lambda_i^2$  of the matrix  $\Omega^2$  can be obtained by writing down the characteristic polynomial  $p(\lambda^2) \equiv \det(\Omega^2 - \lambda^2)$  of  $\Omega^2$ . Denoting the determinant of the  $k \times k$  upper-left submatrix of  $\Omega^2 - \lambda^2$  as  $p_k$ , then  $p_k$ 's have the recurrence relation

$$p_{k} = \alpha_{k} p_{k-1} - \beta_{k},$$

$$\alpha_{k} \equiv \left(\Omega_{kk}^{2} - \lambda^{2}\right),$$

$$\beta_{k} \equiv \Omega_{1k}^{2} \Omega_{k1}^{2} \prod_{i=1}^{k-1} \left(\Omega_{ii}^{2} - \lambda^{2}\right),$$
(B7)

which has the solution

$$p_{k} = \prod_{i=2}^{k} \alpha_{i} p_{1} - \sum_{i=2}^{k} \left( \beta_{i} \prod_{j=i+1}^{k} \alpha_{j} \right)$$

$$= \prod_{i=1}^{k} \left( \Omega_{ii}^{2} - \lambda^{2} \right) - \sum_{i=2}^{k} \Omega_{1i}^{2} \Omega_{i1}^{2} \left[ \prod_{j=2}^{i-1} \left( \Omega_{jj}^{2} - \lambda^{2} \right) \right] \left[ \prod_{j=i+1}^{k} \left( \Omega_{jj}^{2} - \lambda^{2} \right) \right]$$

$$= \left( \prod_{i=1}^{k} \left( \Omega_{ii}^{2} - \lambda^{2} \right) \right) \left( 1 - \sum_{j=2}^{k} \frac{\Omega_{1j}^{2} \Omega_{j1}^{2}}{(\Omega_{11}^{2} - \lambda^{2}) (\Omega_{jj}^{2} - \lambda^{2})} \right)$$

$$= \left( \prod_{i=1}^{k} \left( \omega_{i}^{2} - \lambda^{2} \right) \right) \left( 1 - g^{2} \sum_{j=2}^{k} \frac{|D_{1,j}|^{2} \omega \omega_{j}}{(\omega^{2} - \lambda^{2}) (\omega_{j}^{2} - \lambda^{2})} \right). \tag{B8}$$

In particular,

$$p(\lambda^{2}) \equiv p_{l} = \left(\prod_{i=1}^{l} \left(\omega_{i}^{2} - \lambda^{2}\right)\right) \left(1 - g^{2} \sum_{j=2}^{l} \frac{|D_{1,j}|^{2} \omega \omega_{j}}{(\omega^{2} - \lambda^{2})(\omega_{j}^{2} - \lambda^{2})}\right).$$
(B9)

The eigenvalues  $\lambda_i^2$  are the roots of the equation  $p(\lambda^2) = 0$ . First, consider the case where some of the mean-field eigenenergies are (f+1)-fold degenerate, for example,  $\omega_k = \omega_{k+1} = \cdots = \omega_{k+f}$ , then  $\lambda^2 = \omega_k^2$  is a root of  $p(\lambda^2)$  with multiplicity f, because now the first factor of  $p(\lambda^2)$ ,  $\prod_{i=1}^l (\omega_i^2 - \lambda^2)$ , contains  $(\omega_k^2 - \lambda)^{f+1}$  and  $(\omega_k^2 - \lambda)(1 - g^2 \sum_{j=2}^l \frac{|D_{1,j}|^2 \omega \omega_j}{(\omega^2 - \lambda^2)(\omega_j^2 - \lambda^2)})$  is analytic at  $\lambda^2 = \omega_k^2$ . The components  $v_i$  of an eigenvector  $v \equiv (v_1, v_2, \ldots, v_l)$  corresponding to this root are determined by the following equations:

$$v_i = 0$$
 if  $i < k$  or  $i > k + f$ , (B10)

and

$$\sum_{i=k}^{k+f} |D_{1,i}| v_i = 0.$$
 (B11)

The f solutions of the equations above involve only atom degrees of freedom because  $v_1 = 0$ . They are "dark states" not interacting with the photons. The only atom state v' with mean-field energy  $\epsilon_k$  that interacts with the photons has the vector components

$$v_i' = \begin{cases} 0 & \text{if } i < k \text{ or } i > k + f \\ \frac{|D_{1,i}|}{\sqrt{\sum_{i=k}^{k+f} |D_{1,i}|^2}} & \text{if } k \leqslant i \leqslant k + f. \end{cases}$$
(B12)

And the coupling strength between this state and the photons is  $g\sqrt{\omega\omega_k\sum_{i=k}^{k+f}|D_{1,i}|^2}$ . Therefore, when we encounter dark states that we are not interested in, we can always reduce the dimension of  $\Omega^2$  to a smaller l by removing degenerate mean-field states and renormalizing the atom-photon coupling strength such that the resulting  $\Omega^2$  does not possess eigenvalues equaling certain  $\omega_k^2$ . In this case, the characteristic equation  $p(\lambda^2)=0$  is equivalent to

$$q(\lambda^2) := \omega^2 - \lambda^2 - g^2 \sum_{i=2}^{l} \frac{|D_{1,i}|^2 \omega \omega_i}{\omega_j^2 - \lambda^2} = 0.$$
 (B13)

The function  $q(\lambda^2)$  has simple poles at  $\lambda^2 = \omega_k^2$ ,  $k=2,3,\ldots,l$  and  $q(\omega_j^2\pm 0) \to \pm \infty$ . Also,  $q(\pm \infty) \to \pm \infty$ .  $q(\lambda^2)$  is monotonically decreasing within each interval  $(-\infty,\omega_2^2),(\omega_2^2,\omega_3^2),\cdots,(\omega_{l-1}^2,\omega_l^2),(\omega_l^2,+\infty)$ , supposing  $\omega_2^2 < \omega_3^2 < \cdots < \omega_l^2$ . Therefore  $\lambda_1^2 \in (-\infty,\omega_2^2)$ ,

$$\lambda_2^2 \in (\omega_2^2, \omega_3^2), \dots, \lambda_{l-1}^2 \in (\omega_{l-1}^2, \omega_l^2), \qquad \lambda_l^2 \in (\omega_l^2, +\infty).$$
Note that if  $\omega < \omega_2$ ,  $q(\omega^2) = -g^2 \sum_{j=2}^l \frac{|D_{1,j}|^2 \omega \omega_j}{\omega_j^2 - \omega^2} < 0$ , so  $\lambda_1^2 \in (-\infty, \min(\omega^2, \omega_2^2)).$ 

Because it is meaningless if  $H_{\rm eff}$  has imaginary eigenvalues, it is required that  $\lambda_1^2 \geqslant 0$ , while the positivity of the other eigenvalues of  $\Omega^2$  is automatically guaranteed because they are greater than  $\omega_2^2$  as we discussed.  $\lambda_1^2 \geqslant 0$  is equivalent to  $q(0) \geqslant 0$ , that is,

$$g^2 \sum_{i=2}^{l} \frac{|D_{1,j}|^2}{\omega_j} \leqslant \omega. \tag{B14}$$

By taking the equal sign, we encounter the critical condition derived by the mean-field theory given in Eq. (3). Thus the effective Hamiltonian is consistent with the mean-field theory.

Then, we will calculate the von Neumann entanglement entropy between the atoms and photons in the ground state  $\Phi(\mathbf{X})$  in Eq. (B6). To this purpose, first we calculate the reduced density matrix for the photons:

$$\rho(x_{1}, x_{1}') \equiv \int dx_{2} \cdots dx_{l} \, \Phi(x_{1}, x_{2}, \dots, x_{l}) \Phi^{*}(x_{1}', x_{2}, \dots, x_{l})$$

$$= \left(\frac{\det \Omega}{\pi^{l}}\right)^{1/2} \int dx_{2} \cdots dx_{l} \exp\left(-\sum_{j,k=2}^{l} \Omega_{jk} x_{j} x_{k} - \frac{x_{1} + x_{1}'}{2} \sum_{j=2}^{l} (\Omega_{j1} + \Omega_{1j}) x_{j} - \frac{\Omega_{11}(x_{1}^{2} + x_{1}'^{2})}{2}\right)$$

$$= \left(\frac{\det \Omega}{\pi \det \Omega'}\right)^{1/2} \exp\left(\frac{1}{4} (x_{1} + x_{1}')^{2} \sum_{j,k=2}^{l} \Omega_{1j} \Omega'_{j-1,k-1}^{-1} \Omega_{k1} - \frac{\Omega_{11}(x_{1}^{2} + x_{1}'^{2})}{2}\right), \tag{B15}$$

where  $\Omega'$  is the  $(l-1) \times (l-1)$  lower-right submatrix of  $\Omega$ . Note that

$$\det \Omega = \sum_{j=1}^{l} (-1)^{1+j} \Omega_{1j} M_{1j}$$

$$= \det \Omega' \left( \Omega_{11} - \sum_{j,k=2}^{l} \Omega_{1j} \Omega'_{j-1,k-1}^{-1} \Omega_{k1} \right), (B16)$$

where  $M_{ij}$  is the (i, j)-minor of  $\Omega$ , the determinant of the submatrix of  $\Omega$  that is obtained by removing the *i*th row and

*j*th column from  $\Omega$ ,  $M'_{ij}$  is the (i, j)-minor of  $\Omega'$ , and  $C'_{ij}$  is the (i, j)-cofactor of  $\Omega'$ ,  $C'_{ij} \equiv (-1)^{i+j} M'_{ij}$ . We have used the fact that the inverse of  $\Omega'$  can be expressed through its cofactor:

$$\Omega_{ij}^{\prime-1} = C_{ji}^{\prime} / \det \Omega^{\prime}. \tag{B17}$$

Then using Eq. (B16), the reduced density matrix can be written as

$$\rho(x_1, x_1') = \left(\frac{\det \Omega}{\pi \det \Omega'}\right)^{1/2} \exp\left(\frac{1}{4}(x_1 + x_1')^2 \left(\Omega_{11} - \frac{\det \Omega}{\det \Omega'}\right) - \frac{\Omega_{11}(x_1^2 + x_1'^2)}{2}\right)$$

$$= \left(\frac{\det \Omega}{\pi \det \Omega'}\right)^{1/2} \exp\left(-\frac{1}{2}A^+(x_1^2 + x_1'^2) + A^-x_1x_1'\right), \tag{B18}$$

where  $A^{\pm} \equiv \frac{1}{2}(\Omega_{11} \pm \frac{\det \Omega}{\det \Omega'})$ . The von Neumann entropy S is defined as

$$S = -\text{Tr}(\rho \ln \rho). \tag{B19}$$

To calculate the entanglement entropy, we need to know the eigenvalues of  $\rho$ . To this purpose, comparing  $\rho$  with the propagator of a one-dimensional harmonic oscillator

$$\langle x_1 | \exp\left(-\frac{P_1^2 + \gamma^2 X_1^2}{2}\right) | x_1' \rangle = \sqrt{\frac{\gamma}{2\pi \sinh \gamma}} \exp\left(\frac{\gamma \left(-\cosh \gamma \left(x_1^2 + x_1'^2\right) + 2x_1 x_1'\right)}{2 \sinh \gamma}\right), \tag{B20}$$

we can identify

$$\cosh \gamma = \frac{A^+}{A^-},\tag{B21}$$

such that the eigenvalues of  $\rho$  is given by  $2\sinh(\frac{\gamma}{2})\exp(-\gamma(k+\frac{1}{2})), \quad \gamma > 0, \ k=0,1,2,\ldots$  Now the atom-photon entanglement entropy can be obtained as follows:

$$S = \frac{\gamma}{e^{\gamma} - 1} - \ln(1 - e^{-\gamma}). \tag{B22}$$

So the entanglement entropy is determined by a single parameter  $\gamma$ . The parameter  $\gamma$  can be extracted from the measurement of photon quadrature fluctuations. Note that

$$\langle X_1^2 \rangle = \int x^2 \rho(x, x) dx$$

$$= \left( \frac{\det \Omega}{\pi \det \Omega'} \right)^{1/2} \int x^2 \exp\left( -\frac{\det \Omega}{\det \Omega'} x^2 \right) dx$$

$$= \frac{M_{11}}{2 \det \Omega},$$
(B23)

- [1] R. H. Dicke, Phys. Rev. 93, 99 (1954).
- [2] F. Dimer, B. Estienne, A. S. Parkins, and H. J. Carmichael, Phys. Rev. A 75, 013804 (2007).
- [3] D. Nagy, G. Kónya, G. Szirmai, and P. Domokos, Phys. Rev. Lett. 104, 130401 (2010).
- [4] K. Baumann, C. Guerlin, F. Brennecke, and T. Esslinger, Nature (London) 464, 1301 (2010).
- [5] Z. Zhang, C. H. Lee, R. Kumar, K. J. Arnold, S. J. Masson, A. L. Grimsmo, A. S. Parkins, and M. D. Barrett, Phys. Rev. A 97, 043858 (2018).
- [6] A. Safavi-Naini, R. J. Lewis-Swan, J. G. Bohnet, M. Gärttner, K. A. Gilmore, J. E. Jordan, J. Cohn, J. K. Freericks, A. M. Rey, and J. J. Bollinger, Phys. Rev. Lett. 121, 040503 (2018).
- [7] L. Lamata, Sci. Rep. 7, 43768 (2017).
- [8] A. Mezzacapo, U. Las Heras, J. Pedernales, L. DiCarlo, E. Solano, and L. Lamata, Sci. Rep. 4, 7482 (2014).
- [9] N. Langford, R. Sagastizabal, M. Kounalakis, C. Dickel, A. Bruno, F. Luthi, D. Thoen, A. Endo, and L. DiCarlo, Nat. Commun. 8, 1715 (2017).
- [10] X. Li, M. Bamba, N. Yuan, Q. Zhang, Y. Zhao, M. Xiang, K. Xu, Z. Jin, W. Ren, G. Ma, S. Cao, D. Turchinovich, and J. Kono, Science 361, 794 (2018).
- [11] S. J. Masson, M. D. Barrett, and S. Parkins, Phys. Rev. Lett. 119, 213601 (2017).
- [12] Z. Zhiqiang, C. H. Lee, R. Kumar, K. J. Arnold, S. J. Masson, A. S. Parkins, and M. D. Barrett, Optica 4, 424 (2017).
- [13] Y.-Q. Zou, L.-N. Wu, Q. Liu, X.-Y. Luo, S.-F. Guo, J.-H. Cao, M. K. Tey, and L. You, Proc. Natl. Acad. Sci. USA 115, 6381 (2018).
- [14] T. S. Chang, A. Hankey, and H. E. Stanley, Phys. Rev. B 8, 346 (1973)
- [15] A. Hankey, H. E. Stanley, and T. S. Chang, Phys. Rev. Lett. 29, 278 (1972).

and

$$\begin{split} \left\langle P_{1}^{2}\right\rangle &=-\int \left.\frac{\partial^{2}\rho(x,x')}{\partial x^{2}}\right|_{x'=x} dx \\ &=-\int \left[\left(\frac{\det\Omega}{\det\Omega'}\right)^{2}x^{2}-A^{+}\right]\rho(x,x)dx \\ &=A^{+}-\frac{\det\Omega}{2\det\Omega'}=\frac{\Omega_{11}}{2}. \end{split} \tag{B24}$$

We also have

$$\langle X_1^2 \rangle = \frac{\langle (b_1 + b_1^{\dagger})^2 \rangle}{2\omega},\tag{B25}$$

and

$$\langle P_1^2 \rangle = -\frac{\omega}{2} \langle (b_1^{\dagger} - b_1)^2 \rangle.$$
 (B26)

So

$$\gamma = \cosh^{-1}\left(\frac{\zeta+1}{\zeta-1}\right),\tag{B27}$$

$$\zeta \equiv \frac{\Omega_{11} M_{11}}{\det \Omega} = -\langle (b_1 + b_1^{\dagger})^2 \rangle \langle (b_1^{\dagger} - b_1)^2 \rangle, \quad (B28)$$

where  $b_1 + b_1^{\dagger}$  and  $b_1^{\dagger} - b_1$  are so-called quadrature operators.

- [16] R. B. Griffiths, Phys. Rev. B 12, 345 (1975).
- [17] G. F. Tuthill, J. F. Nicoll, and H. E. Stanley, Phys. Rev. B 11, 4579 (1975).
- [18] E. K. Riedel, Phys. Rev. Lett. 28, 675 (1972).
- [19] T. Chang, D. Vvedensky, and J. Nicoll, Phys. Rep. 217, 279 (1992).
- [20] R. B. Griffiths, Phys. Rev. Lett. 24, 715 (1970).
- [21] K. Rzażewski, K. Wódkiewicz, and W. Żakowicz, Phys. Rev. Lett. 35, 432 (1975).
- [22] I. Bialynicki-Birula and K. Rzażewski, Phys. Rev. A 19, 301 (1979).
- [23] A. Vukics and P. Domokos, Phys. Rev. A 86, 053807 (2012).
- [24] A. Vukics, T. Grießer, and P. Domokos, Phys. Rev. Lett. 112, 073601 (2014).
- [25] D. Campbell, R. Price, A. Putra, A. Valdés-Curiel, D. Trypogeorgos, and I. Spielman, Nat. Commun. 7, 10897 (2016).
- [26] Y. Xu and H. Pu, Phys. Rev. Lett. 122, 193201 (2019).
- [27] H.-J. Zhu, K. Xu, G.-F. Zhang, and W.-M. Liu, Phys. Rev. Lett. 125, 050402 (2020).
- [28] F. Gerbier, A. Widera, S. Fölling, O. Mandel, and I. Bloch, Phys. Rev. A 73, 041602(R) (2006).
- [29] S. R. Leslie, J. Guzman, M. Vengalattore, J. D. Sau, M. L. Cohen, and D. M. Stamper-Kurn, Phys. Rev. A 79, 043631 (2009).
- [30] E. M. Bookjans, A. Vinit, and C. Raman, Phys. Rev. Lett. 107, 195306 (2011).
- [31] C. Cohen-Tannoudji and J. Dupont-Roc, Phys. Rev. A 5, 968 (1972).
- [32] L. Santos, M. Fattori, J. Stuhler, and T. Pfau, Phys. Rev. A **75**, 053606 (2007).
- [33] K. Jensen, V. M. Acosta, J. M. Higbie, M. P. Ledbetter, S. M. Rochester, and D. Budker, Phys. Rev. A 79, 023406 (2009).

- [34] A. de Paz, A. Sharma, A. Chotia, E. Maréchal, J. H. Huckans, P. Pedri, L. Santos, O. Gorceix, L. Vernac, and B. Laburthe-Tolra, Phys. Rev. Lett. 111, 185305 (2013).
- [35] L.-M. Duan, G. Giedke, J. I. Cirac, and P. Zoller, Phys. Rev. Lett. **84**, 2722 (2000).
- [36] V. Josse, A. Dantan, A. Bramati, and E. Giacobino, J. Opt. B Quantum Semiclassical Opt. 6, S532 (2004).
- [37] J. Vidal and S. Dusuel, Europhys. Lett. 74, 817 (2006).
- [38] J. Vidal, S. Dusuel, and T. Barthel, J. Stat. Mech.: Theory Exp. (2007) P01015.